Progress In Electromagnetics Research C, Vol. 83, 57–70, 2018

Design of a Novel Compact and Efficient Rectenna For WiFi Energy Harvesting

Yanyan Shi, Jianwei Jing, Yue Fan, Lan Yang, and Meng Wang*

Abstract—With the increase of low power devices, the design of a compact and efficient rectenna is essential for supplying energy to the devices. This paper presents a compact rectenna for high efficient WiFi energy harvesting. A novel fractal geometry is introduced in the design of antenna for miniaturization, and the ability to harvest WiFi energy is enhanced due to its characteristics of self-similarity and space filling. Besides, a single stub matching network is designed to achieve high conversion efficiency with a relatively low input power ranging from −20 dBm to 0 dBm. Simulation and experiments have been carried out. The results show that the proposed antenna features a good characteristic of reflection coefficient and realized gain at WiFi band. The highest RF to DC conversion efficiency of the rectenna is up to 52% at 2.45 GHz with the input power of 0 dBm. This study demonstrates that the proposed rectenna can be applied to a range of low power electronic applications.

1. INTRODUCTION

In recent years, wireless communication has undergone dramatic development. An increasing number of radio transmitters are available in the ambient environment such as mobile base stations, digital TV towers and WiFi routers. The wide availability of RF signals provides an alternative solution to power low-power electronic device without the needs of batteries [1, 2]. However, the RF power obtained from the environment is usually at the scale of milli-watts or micro-watts which is a critical problem that limits the popularity of the RF energy harvest. In order to maximize the harvested energy, the rectenna which consists of antenna and rectifier is crucial in the process of energy harvesting.

A variety of rectennas have been designed and investigated for RF energy harvesting. Energy conversion efficiency of RF to DC is a vital parameter to evaluate the performance of rectennas. High conversion efficiency can be achieved by monopole rectennas [3–5]. However, these retennas are generally designed at a single frequency band, and high power density is required. To harvest more ambient RF energy from multiple frequency bands, a reasonable solution is to use a multiband or broadband antenna array which is able to operate at low power density [6–12]. However, the multiband or broadband antenna array usually has a large dimension, and the complex structure of the array may result in coupling between the antenna elements which reduces the efficiency of the elements. To address this problem, fractal antennas with different geometries such as Koch snowflake, Minkowski-like and Sierpinski triangle are applied in the design of rectenna to increase effective electrical length [13–15]. In [16], a compact fractal loop rectenna is presented to capture RF energy at 1.8 GHz, but the realized gain is relatively low. In [17], an ultra-compact low-power rectenna for RF energy harvesting in WiFi band is presented. However, the RF-DC conversion efficiency is not very high. In reality, radio transmitters such as WiFi router usually transmit electromagnetic wave with random polarization. Correspondingly, omnidirectional antennas are proposed for ambient RF energy harvest. However, their realized gains normally distribute evenly in all directions which results in a low realized gain

Received 28 January 2018, Accepted 21 March 2018, Scheduled 9 April 2018
* Corresponding author: Meng Wang (wangmeng@htu.edu.cn).
The authors are with the Department of Electronic and Electrical Engineering, Henan Normal University, Xinxiang 453007, China.

and reduces the ability of harvesting RF energy at a relatively far distance. A directional antenna is presented to obtain a higher gain towards a specific direction, and more RF energy can be captured even at farther distance [18–20]. The rectifier is also essential to the design of the rectenna, which determines how much input RF energy will be converted into DC power. Greinacher rectifier circuit is a popular topology for wireless power transmission. To enhance the conversion efficiency of rectifier circuit with a fixed load resistance at low input power levels, a matching network is of great importance [21–24].

In this paper, a compact fractal rectenna is proposed to harvest the ambient RF energy working in the range of 2.4 GHz to 2.48 GHz. First, fractal geometry is introduced in the design of antenna patch for miniaturization, and the performances of fractal antennas with four different numbers of corners are studied and compared. Further, antenna with better performance is obtained by investigating the impact of the radius of the circumscribed circle of the fractal patch. A voltage doubler rectifier is employed to realize the conversion of RF to DC, and an optimal load resistance is obtained. Additionally, a novel stub matching network is designed to improve the overall efficiency of rectenna at low input power. Finally, experimental measurements are carried out to evaluate the performance of the proposed rectenna.

2. DESIGN OF THE FRACTAL RECTENNA

A block diagram of the rectenna for harvesting ambient RF energy in the WiFi band is shown in Fig. 1. Ambient WiFi energy is harvested by the rectenna which consists of an antenna for capturing the ambient WiFi energy and a rectifier for converting the RF power into DC power with a matching network to deliver the maximum RF energy for rectifier circuit. The captured energy from the rectenna is then supplied to miniature and low-power electronic devices.

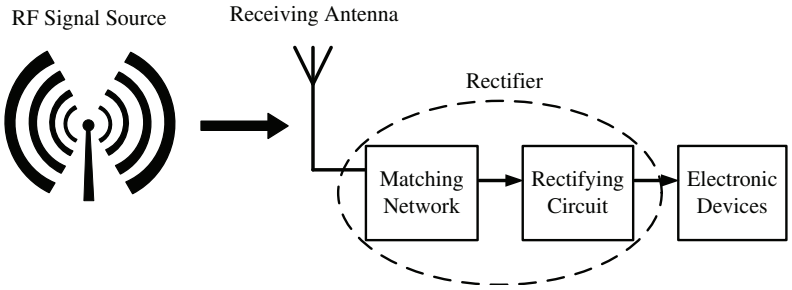

Figure 1. Block diagram of rectenna for ambient RF energy harvesting at WiFi band.

The maximum transmitting power of a typical WiFi router is 100 mW, and the power is lower than 0 dBm at a specific direction due to the omnidirection of the transmitting antennas. Therefore, it is vital that the rectenna is designed to be more efficient for the harvest of WiFi energy at low power levels. In addition, the rectenna should be compact for displacement in small-sized devices.

2.1. The Fractal Antenna Design

Due to the requirement of the low-power devices in terms of miniaturization, a microstrip antenna using coaxial probe feed technique is generally employed which consists of radiating patch, substrate and ground plane, as shown in Fig. 2.

In this paper, a novel fractal antenna is proposed which provides an alternative method to minimize the microstrip antenna. Based on the self-similarity of fractal theory, the proposed fractal geometry is designed as illustrated in Fig. 3. It consists of multiple bending curves as shown in Fig. 3(a). Then other multiple bending curves are made to be symmetric about the line $y = -\sqrt{3}x$, and a straight line d_3 is used for a closed structure. The proportional relationship between the radius and segment length can be expressed as:

$$2r_1 = 8r_2 = 8r_3 = 4r_4 = 2r_5 = r_6 = \frac{4}{3}r_7 = r_8 = d_1 = \frac{4}{3}d_2 = \frac{4}{29}d_3 \tag{1}$$

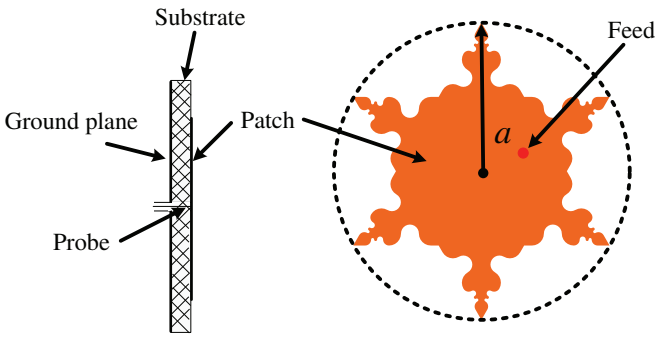

Figure 2. Structure of the fractal microstrip antenna.

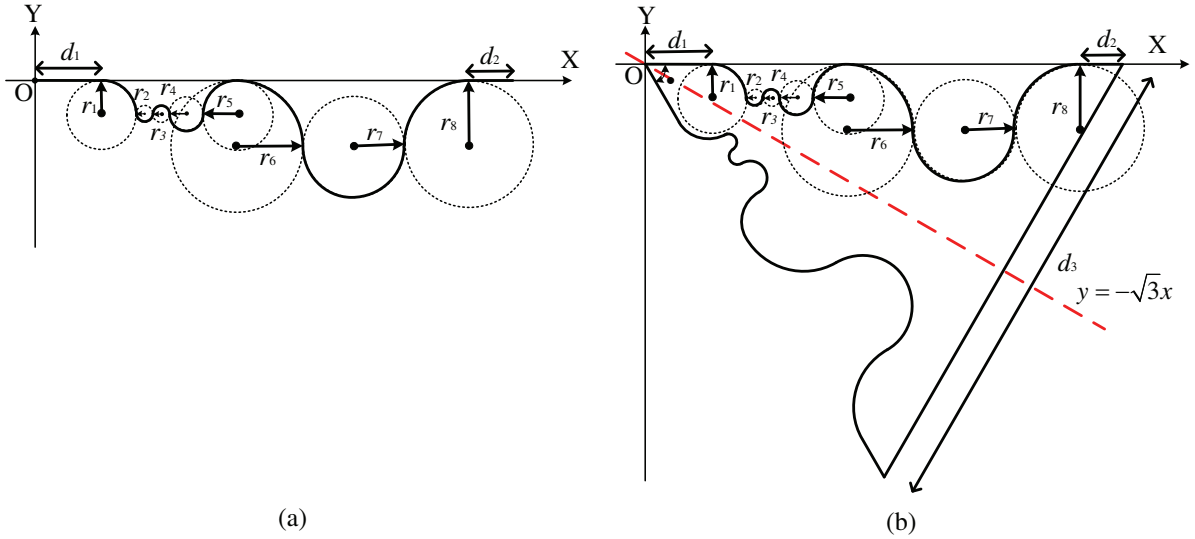

Figure 3. Fractal geometry of radiating patch. (a) Generation of the multiple bending curve; (b) Generation of the fractal geometry.

Based on Fig. 3, fractal antennas with the same radius of the circumscribed circle ($a = 18.2\,\text{mm}$) are designed as shown in Fig. 4. Considering the accuracy of the manufacture, fractal patch with four different numbers of corners ($N = 4$, 6, 8 and 10) are investigated and compared. The relationship between the side length of polygons $d_{3\_N=4}$, $d_{3\_N=6}$, $d_{3\_N=8}$, $d_{3\_N=10}$ and a can be expressed as:

$$d_{3\_N=4} = \frac{2a}{\sqrt{3}+1},\ dd_{3\_N=6} = \frac{\sqrt{3}}{3}a,\ dd_{3\_N=8} = \frac{2a}{\sqrt{3}+\tan\dfrac{3\pi}{8}},\ dd_{3\_N=10} = \frac{2a}{\sqrt{3}+\tan\dfrac{2\pi}{5}} \tag{2}$$

The microstrip antenna can be equivalent to an RLC circuit as depicted in Fig. 5, where R is the resonance resistance, L the equivalent inductance, C the equivalent capacitance between the radiation patch and substrate, and X_L the equivalent inductive reactance caused by the probe.

The relationship between the input impedance Z_{in} of the equivalent circuit and frequency f can be calculated by:

$$Z_{in} = \frac{R}{1+Q_T^2\left(\dfrac{f}{f_r}-\dfrac{f_r}{f}\right)^2} - j\left(\frac{RQ_T\left(\dfrac{f}{f_r}-\dfrac{f_r}{f}\right)}{1+Q_T^2\left(\dfrac{f}{f_r}-\dfrac{f_r}{f}\right)^2} - X_L\right) \tag{3}$$

where Q_T is a quality factor of the circuit, and f_r is the resonance frequency.

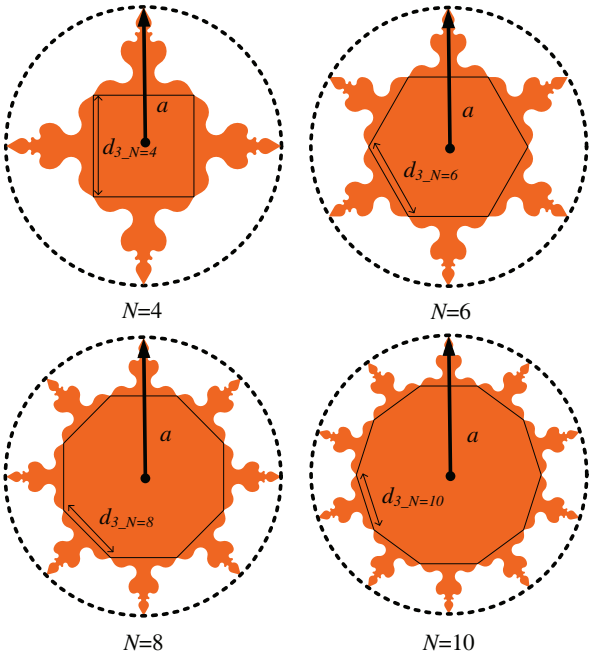

Figure 4. Structure of fractal radiating patches with different number of corners.

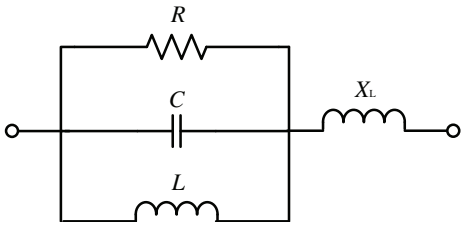

Figure 5. Equivalent circuit of microstrip antenna.

The resonance frequency f_r can be estimated by [25]

$$f_r = \frac{1.841c}{\pi r\sqrt{\varepsilon_r}} \tag{4}$$

where c is the speed of light, and ε_r is the relative permittivity of the substrate.

The reflection parameter Γ of the antenna can be estimated by:

$$\Gamma = \frac{Z_{in} - Z_0}{Z_{in} + Z_0} \tag{5}$$

where Z_0 is the standard impedance of antenna.

From Eq. (3) and Eq. (5), it can be drawn that the input impedance and reflection parameter are related to the equivalent parameters of the microstrip antenna and the external frequency. For optimal performance, the antenna should be designed to operate at the resonant state.

The structure of the proposed antenna is shown in Fig. 6. The antenna has two FR_4 substrates with a relative permittivity of 4.4. The radiating patch of the fractal antenna is printed on the top substrate. Generally, the coaxial feed will generate a narrow frequency band. In order to increase the bandwidth of antenna and reduce the mutual coupling between the fractal radiating patch and ground plane, four helical patches are built on the top layer of the bottom substrate. The proposed antenna which includes a fractal patch and four helical patches is designed at resonant mode. The overall dimension of the fractal antenna is $38 \times 38 \times 3.2\,\text{mm}^3$. Design parameters of the proposed antennas are listed in Table 1.

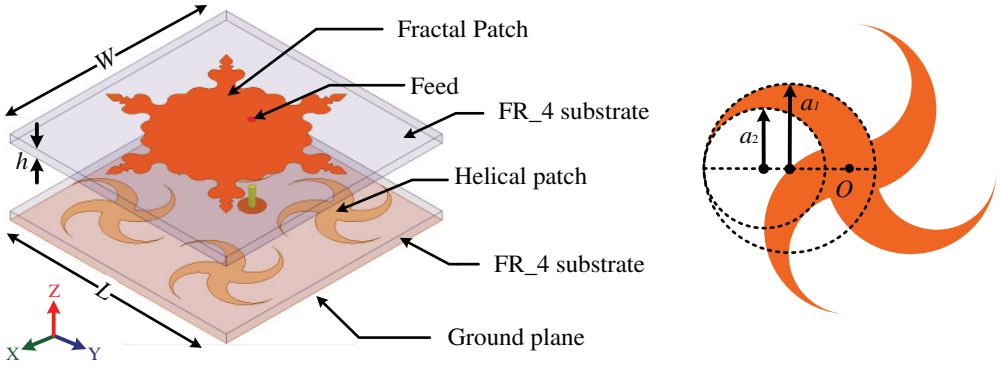

Figure 6. Geometry of the proposed fractal antenna.

Table 1. Parameters of the proposed antenna.

Parameters	W	L	h	a_1	a_2
Value (mm)	38	38	1.6	5	3.5

The performances of fractal antennas are studied and compared in Fig. 7 using ANSYS HFSS13.0. The boundary of the ground plane, fractal patch and the four helical patches is set up to be perfect E, and the boundary of the air box is radiation. A wave port is selected as an excitation, and excitation source of mode 1 is used in the port. As shown in Fig. 7(a), with the increment of N, the resonance frequency gradually decreases as 2.605 GHz, 2.454 GHz, 2.402 GHz and 2.359 GHz, respectively, and the minimum value of reflection coefficient $|S_{11}|$ tends to be smaller. It should also be noted that these antennas operate at four different frequency bands when $|S_{11}| < -10$ dB which are 2.55–2.65 GHz for $N = 4$, 2.42–2.5 GHz for $N = 6$, 2.36–2.44 GHz for $N = 8$ and 2.32–2.4 GHz for $N = 10$. From Fig. 7(b), it can be observed that realized gain varies from -2.5 dBi to 3.8 dBi in the range of frequency bands and gradually increases at the center frequency of WiFi band. The radiation patterns of the four antennas in two principal planes, E-plane (xoy) and H-plane (yoz) at 2.45 GHz, are presented in Fig. 7(c). It is found that the radiation characteristics of the four fractal antennas are relatively symmetrical at E-plane and concentrated mostly along the positive z-axis with a low back-lobe within -3.8 dBi. The peak realized gains of the four fractal antennas are incremental with N at the angle of 0°. Furthermore, the maximum realized gain at H-plane distributes evenly which enhances the ability of the proposed antenna for RF energy harvest. From the analysis above, the summarized parameters along with impedance and VSWR of the proposed antennas are listed in Table 2. It can be easily observed that the antenna with $N = 6$ is optimal for ambient WiFi energy harvest.

The radius of the circumscribed circle of the fractal patch has a significant impact on the performance of the antenna. In order to make the proposed antenna more suitable for WiFi energy harvest, the impact of the radius of the circumscribed circle is investigated for antenna with $N = 6$, which varies from 18.14 mm to 18.30 mm with a step of 0.4 mm, as depicted in Fig. 8. As shown in Fig. 8(a), with the increase of a, the resonance frequency gradually decreases; the minimum value of

Table 2. Detailed parameters of the proposed antenna.

Antenna	$N = 4$	$N = 6$	$N = 8$	$N = 10$
Resonance Frequency (GHz)	2.605	2.454	2.402	2.359
Reflection Coefficient (dB)	-16	-29	-31	-49
Impedance (Ω)	58.2	50.1	51.9	50.1
VSWR	1.6	1.01	1.06	1.01
Realized Gain (dBi)	2.4	2.8	3.1	3.1

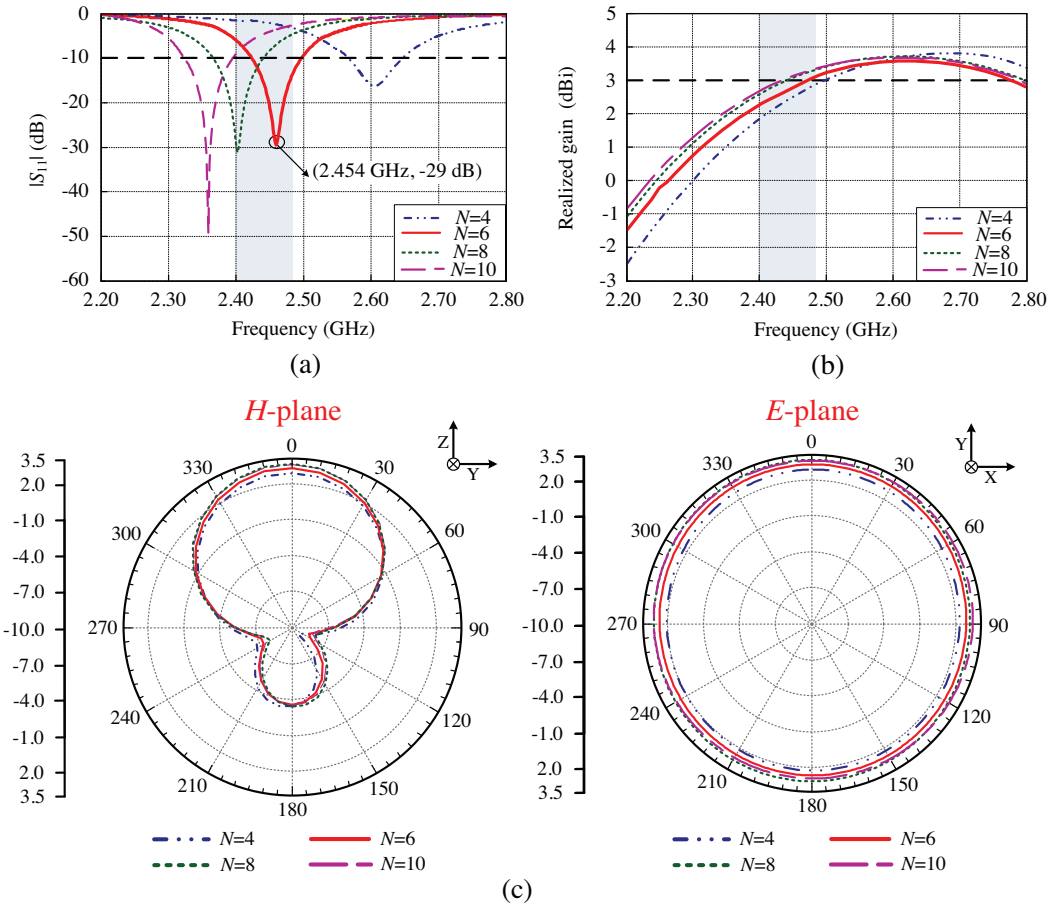

Figure 7. Simulated results of antenna with variation of N: (a) reflection coefficients ($|S_{11}|$); (b) realized gain; (c) radiation pattern in H-plane and E-plane. The band of WiFi (2.4–2.48 GHz) is marked with yellow stripe.

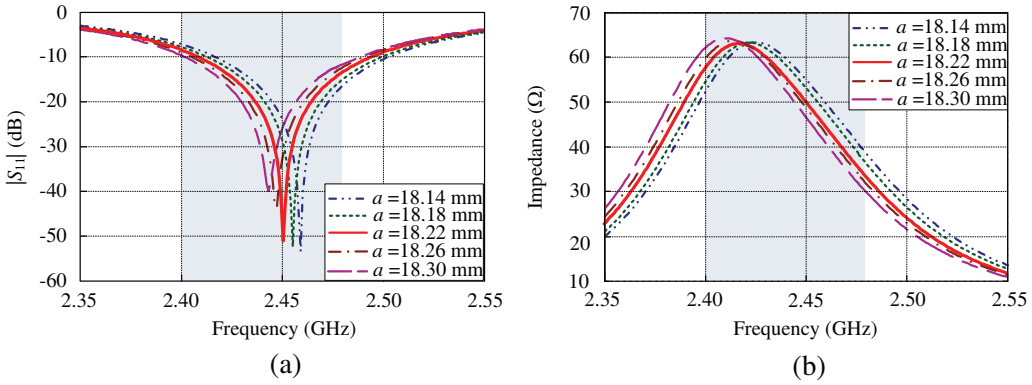

Figure 8. Simulated results of antenna when $N = 6$ with variation of a, (a) reflection coefficients ($|S_{11}|$); (b) impedance.

$|S_{11}|$ varies from −53 dB to −40 dB; the bandwidth gradually approaches WiFi band. Besides, the input impedance of the fractal antenna is investigated using de-embedded method by HFSS simulation. The real part of the input impedance of the antenna versus the variation of a is depicted in Fig. 8(b). It can be noted that the maximum real part of the input impedances gradually moves to lower frequency when a increases. Additionally, the real part of the input impedance decreases at 2.45 GHz with 55 Ω, 52 Ω,

50 Ω, 48 Ω and 47 Ω, respectively. The detailed parameters of the proposed antenna with the variation of a, when $N = 6$, are summarized in Table 3. A conclusion can be drawn that when $a = 18.22$ mm, the antenna is the most appropriate alternative with the resonance frequency of 2.45 GHz and the standard input impedance of 50 Ω.

Table 3. Comparison of the proposed antenna with the variation of a.

a (mm)	Resonance Frequency (GHz)	Reflection Coefficient (dB)	Impedance (Ω)	Realized Gain (dBi)
18.14	2.459	−53	55	2.72
18.18	2.455	−52	52	2.85
18.22	2.450	−51	50	3.00
18.26	2.447	−43	48	3.12
18.30	2.443	−40	47	3.21

Finally, the performance of the proposed fractal antenna with $a = 18.2$ mm and $a = 18.22$ mm when $N = 6$ is compared in Fig. 9. It can be seen from Fig. 9(a) that resonance frequency varies from 2.454 GHz to 2.45 GHz, and the minimum $|S_{11}|$ decreases from −29 dB to −51 dB. The realized gain increases from 2.6 dBi to 3.0 dBi at 2.45 GHz as shown in Fig. 9(b). Due to the higher realized gain, the antenna can be placed at a farther distance to receive the same power when the transmitted power and gain of the transmitting antenna are fixed. As a result, the optimized antenna has better performance when capturing WiFi energy.

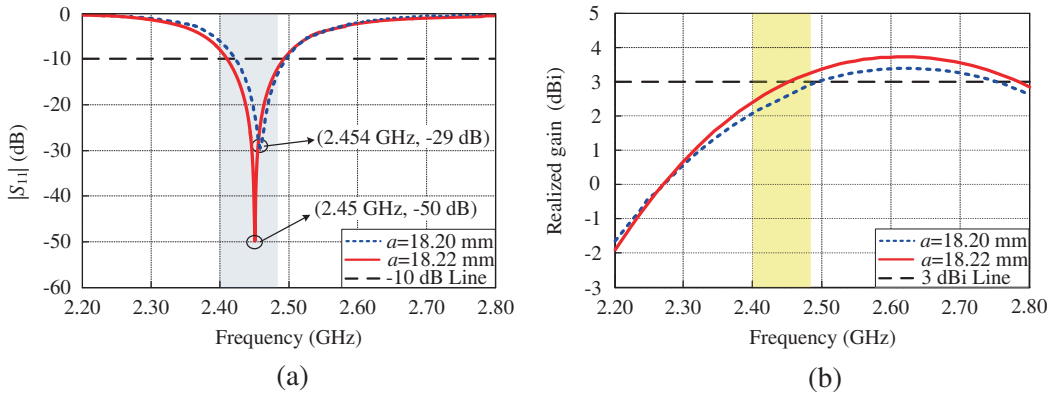

Figure 9. Results of antenna when $N = 6$ for $a = 18.2$ mm and 18.22 mm: (a) reflection coefficients ($|S_{11}|$); (b) realized gain.

2.2. Rectifier Design

The rectifying circuit is also essential in the design of rectenna since it determines the conversion efficiency of RF to DC, as shown in Fig. 10. It is composed of a pair of diodes to realize the conversion of RF to DC, a filter capacitor to store energy and smooth the output DC voltage, and a load. Additionally, the Schottky diode HSMS2852 is chosen due to its low bias input voltage.

The input impedance of the rectifying circuit is affected by the resistance of the load, and there is also a significant impact of the load on the output voltage and conversion efficiency. Besides, there exist an optimal resistance of load and an optimal power within the input power range for the rectifier. The resistance of the load is swept varying from 1 kΩ to 50 kΩ with input power ranging from −20 dBm to 0 dBm by ADS simulation. Co-simulation of harmonic balance and momentum is adopted to investigate the performance of the rectifier when the layout and schematic are co-simulated with simulation. The optimal load resistance of the rectifying circuit is found to be 4 kΩ where the maximum conversion efficiency is 22% at the optimal input power of 0 dBm as given in Fig. 11.

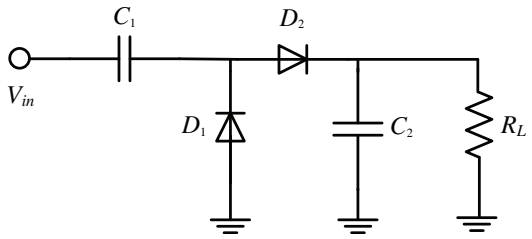

Figure 10. Schematic of a typical voltage doubler rectifying circuit.

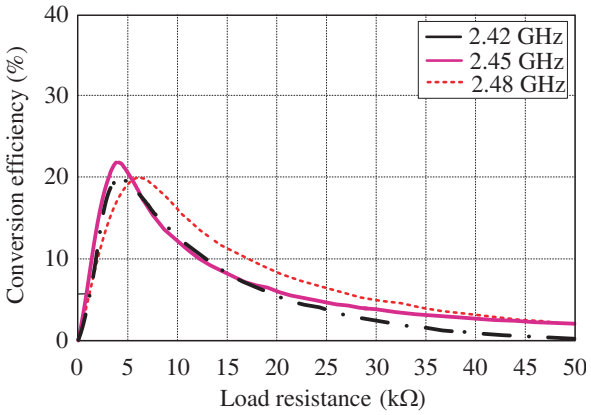

Figure 11. Simulated RF to DC conversion efficiency of the rectifying circuit as a function of load resistance.

In order to enhance the conversion efficiency of rectifying circuit under low input power, an open stub matching network is designed to match the impedance of $16.604 - j * 59.6\Omega$ at 0 dBm, and the layout of the rectifier is shown in Fig. 12.

The reflection coefficient of the stub matching network is shown in Fig. 13. It can be observed that the matching network works well over the frequency bands 2.18 GHz–2.7 GHz when $|S_{11}| < -10$ dB, and the minimum $|S_{11}|$ is -38 dB at 2.45 GHz. For comparison, the performance of the rectifier before and after adding matching network is shown in Fig. 14. It is observed that the maximum efficiency is improved from 22% to 66%, and the efficiency at low input power -10 dBm has also been enhanced

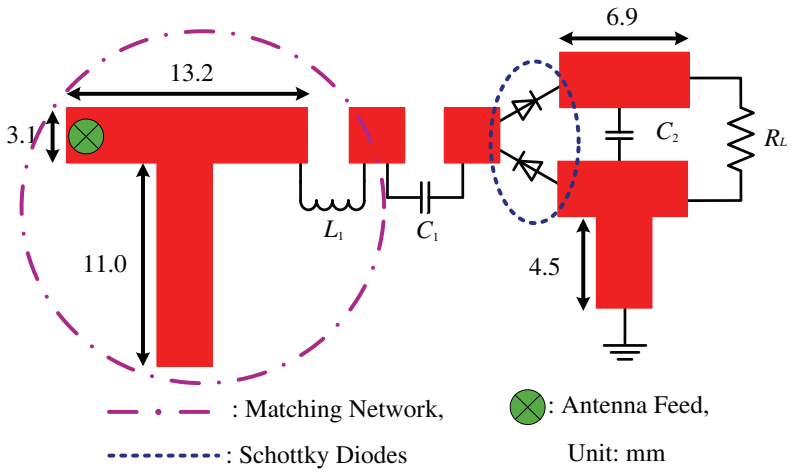

Figure 12. Prototype of the proposed rectifier with an open stub matching network. $L_1 = 4$ nH, $C_1 = 27$ pF, $C_2 = 200$ nF, Diodes: HSMS2852.

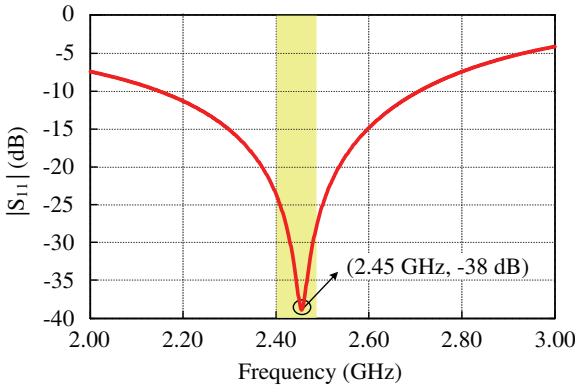

Figure 13. Simulated reflection coefficients ($|S_{11}|$) of the matching network.

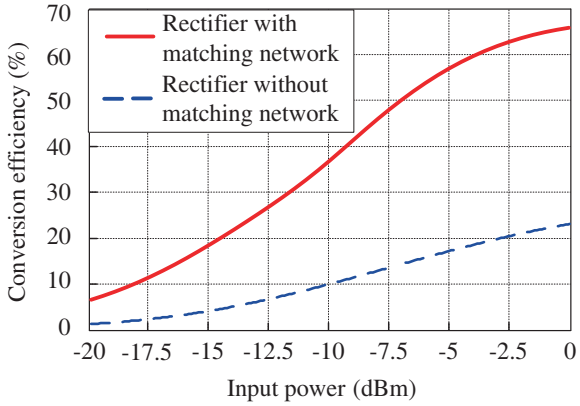

Figure 14. Simulated RF to DC conversion efficiency of the rectifier as a function of input power.

significantly from 10% to 37%. It is demonstrated that the designed matching network greatly enhances the efficiency at low input power.

The performance of the rectifier is shown in Fig. 15 with the variation of frequency and input power. The reflection coefficients at three input power levels are depicted in Fig. 15(a). It can be seen that with the decrease of input power, the matching frequency gradually decreases, and the minimum value of $|S_{11}|$ varies from -32 dB to -16 dB. It can also be found that rectifier has a good impedance matching at WiFi band when the input level varies from -20 dBm to 0 dBm. The RF to DC conversion efficiencies of rectifier against input power at different frequencies are plotted in Fig. 15(b). It can be observed that the conversion efficiency increases gradually with the increase of input power. At the input power of 0 dBm, the conversion efficiency achieves 65%, 66% and 67% at the resonance frequencies of 2.42 GHz, 2.45 GHz and 2.48 GHz, respectively.

3. MEASURED RESULTS AND DISCUSSIONS

In order to validate the performance of the proposed rectenna, experiments have been carried out. Fig. 16 shows the top and bottom views of the fabricated rectenna.

The measured and simulated reflection coefficients and realized gains of the proposed antenna are plotted and compared in Fig. 17. It can be seen from Fig. 17(a) that the measured reflection coefficient reaches the minimum value of -38 dB at 2.48 GHz, and the operating bandwidth of antenna is 2.4 GHz to 2.51 GHz. There exists a small deviation between the simulated and measured reflection coefficients, which is mainly caused by the fabrication tolerance of antenna patch and the error in the relative permittivity of substrate. Besides, it may also be caused by the soldering impact of SMA connector

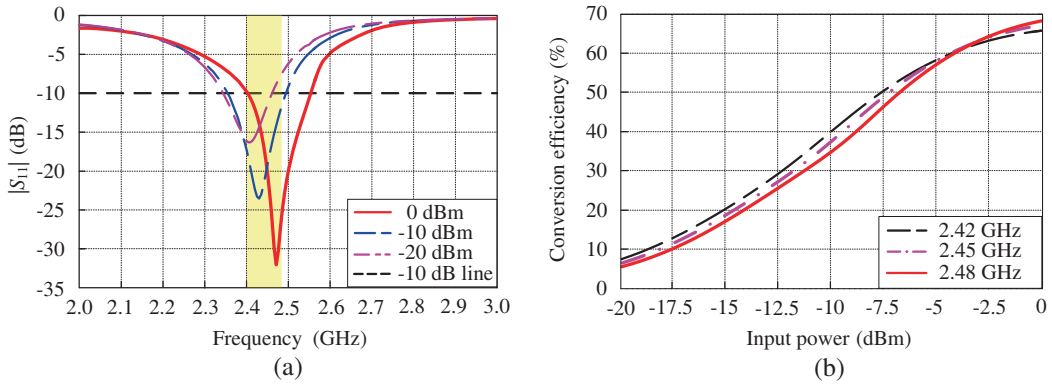

Figure 15. The performance of the rectifier. (a) Simulated $|S_{11}|$ of rectifier for four input power levels. (b) RF to DC conversion efficiency of rectifier at three frequencies.

Figure 16. The photograph of rectenna: (a) top view, (b) bottom view.

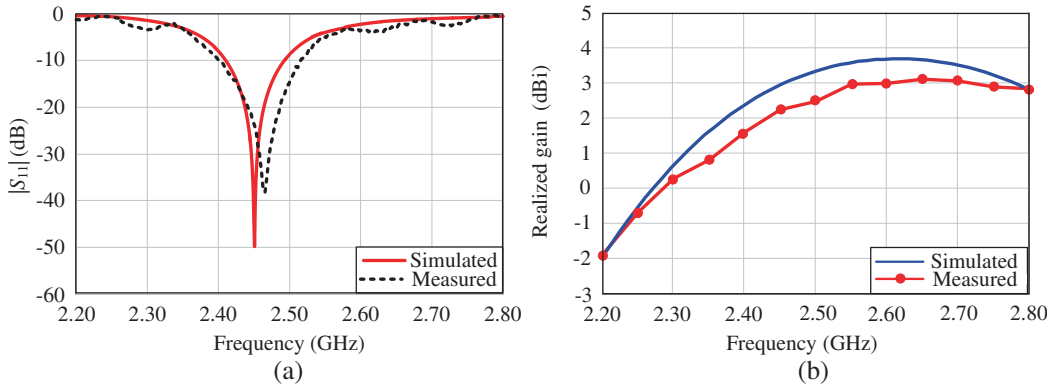

Figure 17. Measured and simulated results of the optimal antenna with $a = 18.22$ when $N = 6$: (a) $|S_{11}|$, (b) the realized gain.

and the influence of the coaxial cable in the measurement. In the measurement of the realized gain of the antenna, two identical antennas are used, of which one antenna is used as the transmitting antenna and the other as the receiving antenna. The distance between the two antennas is at far-field of 60 cm. Considering the power loss L at coaxial cable and SMA connector, the realized antenna gain can be expressed as:

$$G = \frac{1}{2}\left[20\lg\left(\frac{4\pi D}{\lambda}\right) - 10\lg\left(\frac{P_t}{P_r}\right) + L\right] \tag{6}$$

where P_t is the power input to the transmitting antenna from the spectrum analyzer, P_r the received

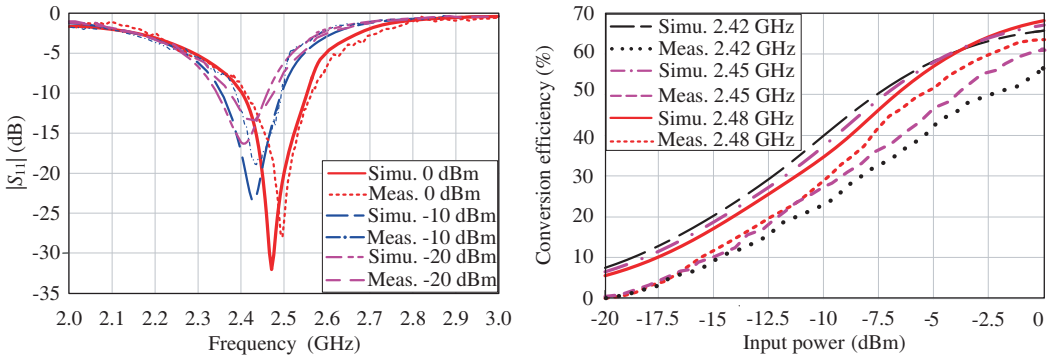

Figure 18. Measured and simulated results of rectifier: (a) $|S_{11}|$, (b) RF to DC conversion efficiency.

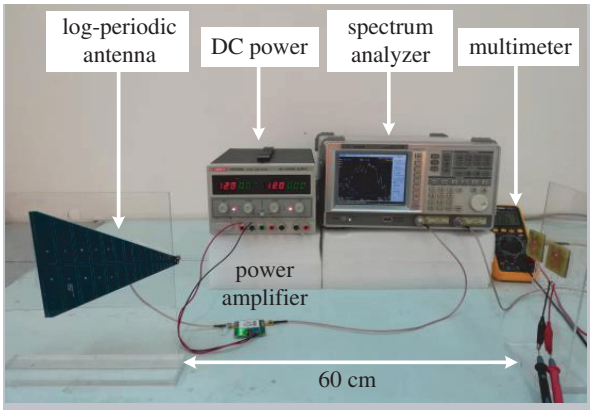

Figure 19. Experimental setup.

power, λ the wavelength, and D the distance between the receiving and transmitting antennas.

Figure 17(b) illustrates the comparison of the simulated and measured realized antenna gains. It can be seen that the measured antenna gain is 2.2 dBi at 2.45 GHz, and the measured realized gain decreases with 0.9 dBi compared with the simulated result at 2.45 GHz. The difference may be caused by the impedance mismatch and polarization mismatch between the two antennas.

Figure 18 shows the performance of the proposed rectifier. The measured and simulated reflection coefficients of the rectifier versus frequency at different input power levels are shown in Fig. 18(a). It can be seen that the measured results agree well with that at the frequency of WiFi band. And the operating frequency of the rectifier for $|S_{11}| < -10$ dB is able to cover the desired WiFi band at three different input power levels -20 dBm, -10 dBm and 0 dBm. It can be concluded that the rectifier performs well at operating frequency under the desired input power levels. In order to evaluate the performance of the proposed rectifier, comparison between the simulated and measured RF to DC conversion efficiency of rectifier with load resistance of 4 kΩ at different input power levels is illustrated in Fig. 18(b). It can be observed that the maximum efficiency varies from 55% to 62% at different frequencies from 2.42 GHz to 2.48 GHz when input power is 0 dBm. The discrepancy between simulated and measured results can be attributed to the nonlinearity of diode and the deviation caused by the unknown parasitic parameters of the SMD components.

In order to evaluate the overall performance of the proposed rectenna, an experimental prototype is set up as shown in Fig. 19. The proposed rectenna and an independent fractal antenna are fabricated and placed at the same distance of 60 cm from transmitting antenna. The rectenna is linked with a multimeter for measuring the output voltage. And the independent antenna is connected with the input port of the spectrum analyzer to evaluate the ability to harvest energy of the proposed antenna.

Besides, a log-periodic broadband antenna with the realized gain of 4 dBi is selected as the transmitting antenna which is connected to the output port of the spectrum analyzer. However, the maximum output power of the spectrum analyzer is only 0 dBm. Therefore, a power amplifier with the gain of 15 dB at 2.4–2.48 GHz is employed to amplified the generated RF signal which is powered by a DC power.

The RF input power level can be varied by changing the transmitting power of the transmitting antenna at a far-field distance $D = 60$ cm, which can be calculated by:

$$P_r = \frac{P_t}{D^2\lambda^2} \times A_{et} \times A_{er} \tag{7}$$

where

$$A_{et}=\frac{G_t\lambda^2}{4\pi} \quad \text{and} \quad A_{er}=\frac{G_r\lambda^2}{4\pi},$$

P_r is the receiving power; P_t is the transmission power; A_{et} and A_{er} are the effective area of transmitting antenna and receiving antenna; G_t and G_r are the antenna gains of the transmitting and receiving antenna, respectively.

The output power of the rectenna can be calculated by:

$$P_{out}=\frac{V_{out}^2}{R_{Load}} \tag{8}$$

where P_{out} is the output power of rectenna, V_{out} the output dc voltage of the load, and R_{Load} the resistance of load.

The conversion efficiency of rectenna can be estimated by:

$$\eta = \frac{P_{\text{out}}}{P_r} \times 100\% = \frac{V_{\text{out}}^2}{R_{\text{Load}}P_r} \times 100\% \tag{9}$$

The measured conversion efficiency of rectenna versus input power at different frequency is given in Fig. 20. It can be observed that the conversion efficiency of rectenna increases gradually with the input power increasing from −20 dBm to 0 dBm and the highest efficiency of the rectenna at the three frequencies are 40% at 2.42 GHz, 52% at 2.45 GHz and 50% at 2.48 GHz, respectively.

The comparison of the performance among the proposed rectenna and some previous reported designs is summarized in Table 4. It can be easily observed that the proposed rectenna features a smaller dimension than the published designs. It can also be found that this work provides a high efficiency of RF to DC, and the measured conversion efficiency at low input power is relatively higher than the majority of rectennnas. Evidently, the proposed rectenna is a good candidate for ambient energy harvest at WiFi band for many electronic applications.

Table 4. Comparison with previous reported rectennas.

Ref.	Frequency (GHz)	Substrate	Dimension (mm^3)	Conversion efficiency at −10 dBm	Maximum conversion efficiency
5	Multi-band 0.9;1.75–2.15;2.45	TLP-5-Taconic	155 × 155 × 7.2	16%	60%
8	Broadband 5.1–5.8/5.8–6.0	R04003C	100 × 160 × 0.803	NA	32%/28%
12	Dual-band 0.915;2.45	RT/Duroid5880	60 × 60 × 60	35%	50%
22	Dual-band 0.9–1.1; 1.8–2.5	Rogers RT6002	120 × 120 × 1.52	20% at 2.4 GHz	45% at 2.4 GHz
This work	**2.45**	**FR_4**	**38 × 38 × 3.2**	**24%**	**52%**

NA: Not available

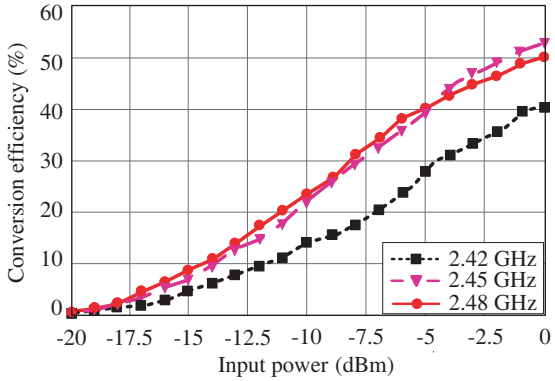

Figure 20. Measured conversion efficiency of rectenna versus input power level at three frequencies.

4. CONCLUSION

A novel compact fractal rectenna has been designed for ambient RF energy harvesting at WiFi band. Antennas with four different numbers of corners are proposed based on fractal geometry. By investigation of reflection coefficient, realized gain and radiation characteristic, when N =6 the antenna is found to be most suitable for WiFi energy harvest. Besides, the optimal radius of the circumscribed circle a of the proposed fractal patch is found to be 18.22 mm at the resonance frequency of 2.45 GHz. A high-efficient rectifier with a stub matching network is designed to maximize the conversion efficiency of RF to DC. The measured results show that the fractal antenna has a minimum reflection coefficient of −38 dB at 2.48 GHz with bandwidth 2.4 to 2.51 GHz, and the realized gain is 2.2 dBi at 2.45 GHz. The maximum conversion efficiency of rectifier is around 62% (at 0 dBm input) at 2.48 GHz. The maximum efficiency of the rectenna is 52% at input power level of 0 dBm with frequency ranging from 2.42 GHz to 2.48 GHz. Compared with other recent designs, the proposed fractal rectenna has a smaller size. In addition, higher efficiency can be obtained at low power level conditions. Owing to the high performance, the proposed rectenna can provide energy to a range of low power electronic devices and wireless sensors by harvesting the ambient low RF power.

ACKNOWLEDGMENT

This work was supported by the Key Science and Technology Project of Henan Province of China (NO. 182102210080) and the Foundation for Key Young Teacher of University by Henan Province of China(NO. 2017GGJS040).

REFERENCES

1. Leclerc, C., M. Egels, and E. Bergeret, "Design and measurement of multi-frequency antennas for RF energy harvesting tags," *Progress In Electromagnetics Research*, Vol. 156, 47–53, 2016.
2. Shaikh, F. K. and S. Zeadally, "Energy harvesting in wireless sensor networks: A comprehensive review," *Renew. Sustain. Energy Rev.*, Vol. 55, 1041–1054, 2016
3. Song, C. Y., Y. Huang, J. Zhou J. Zhang, and S. Yuan, "A high-efficiency broadband rectenna for ambient wireless energy harvesting," *IEEE Transactions on Antennas and Propagation*, Vol. 63, 3486–3495, 2015.
4. Mei, H., X. Yang, B. Han, and G. Tan, "High-efficiency microstrip rectenna for microwave power transmission at Ka band with low cost," *Iet Microwaves Antennas & Propagation*, Vol. 10, 1648–1655, 2016.
5. Masotti, D., A. Costanzo, M. D. Prete, and V. Rizzoli, "Genetic based design of a tetra-band high-efficiency radio-frequency energy harvesting system," *IET Microwave. Antennas Propagat.*, Vol. 7, 1254–1263, 2013.

6. Shin, J., M. Seo, and J. Choi, "A compact and wideband circularly polarized rectenna with high efficiency at X-band," *Progress In Electromagnetics Research*, Vol. 145, 163–173, 2014.
7. Sun, H. and G. Wen, "A new rectenna using beamwidth-enhanced antenna array for RF power harvesting applications," *IEEE Antennas & Wireless Propagation Letters*, 2016.
8. Lu, P., X. S. Yang, and J. L. Li, "Polarization reconfigurable broadband rectenna with tunable matching network for microwave power transmission," *IEEE Trans. Antennas Propag.*, Vol. 64, 1136–1141, 2016 .
9. Gretskih, D. V., A. V. Gomozov, V. A. Katrich, et al., "Mathematical model of large rectenna arrays for wireless energy transfer," *Progress In Electromagnetics Research*, Vol. 74, 77–91, 2017.
10. Kuzu, S. and N. Akcam, "Array antenna using defected ground structure shaped with fractal form generated by apollonius circle," *IEEE Antennas & Wireless Propagation Letters*, Vol. 16, 1020-1023, 2016.
11. Alqadami, A. S. M., M. F. Jamlos, and I. Islam, "Multi-band antenna array based on double negative metamaterial for multi automotive applications," *Progress In Electromagnetics Research*, Vol. 159, 27–37, 2017
12. Sun, H., Y. Guo, M. He, and Z. Zhong, "A dual-band rectenna using broadband Yagi antenna array for ambient RF power harvesting," *IEEE Antennas Wirel. Propag. Lett.*, Vol. 22, 918–921, 2013.
13. Choi, D. Y., S. Shrestha, and S. K. Noh, "Design and performance of an efficient rectenna incorporating a fractal structure," *International Journal of Communication Systems*, Vol. 27, 661–679, 2014
14. Dhaliwal, B. S. and S. S. Pattnaik, "BFOANN ensemble hybrid algorithm to design compact fractal antenna for rectenna system," *Neural Computing & Applications*, Vol. 28, 1–12, 2016.
15. Mahfoudi, H, M. Tellache, and H. Takhedmit, "A wideband fractal rectenna for energy harvesting applications," *2016 10th European Conference on Antennas and Propagation*, 1–4, 2016.
16. Zeng, M., A. Andrenko, and X. Liu, "A compact fractal loop rectenna for RF energy harvesting," *IEEE Antennas and Wireless Propagation*, Vol. 16, 2424–2427, 2017.
17. Palazzi, V., C. Kalialakis, and F. Alimenti, "Performance analysis of a ultra-compact low-power rectenna in paper substrate for RF energy harvesting," *Wireless Sensors & Sensor Networks*, 65–68, 2017.
18. Arrawatia, M., M. S. Baghini, and G. Kumar, "Broadband bent triangular omnidirectional antenna for RF energy harvesting," *IEEE Antennas & Wireless Propagation Letters*, Vol. 15, 36–39, 2016.
19. Shi, Y. and J. Liu, "Wideband and low-profile omnidirectional circularly-polarized antenna with Slits and shorting-vias," *IEEE Antennas & Wireless Propagation Letters*, Vol. 15, 686–689, 2016.
20. Mahmud, M. Z., M. T. Islam, and M. Samsuzzaman, "Design and parametric investigation of directional antenna for microwave imaging application," *Iet Microwaves Antennas & Propagation*, Vol. 11, 770–778, 2017.
21. Song, C. Y., Y. Huang, and P. Carter, "A novel six-band dual CP rectenna using improved impedance matching technique for ambient RF energy harvesting", *IEEE Transactions on Antennas & Propagation*, Vol. 64, 3160–3171 2016.
22. Song, C. Y., Y. Huang, and J. F. Zhou, "Matching network elimination in broadband rectennas for high-ef?ciency wireless power transfer and energy harvesting," *IEEE Transactions on Industrial Electronics*, Vol. 64, 3950–3961, 2017.
23. Kumar, A., S. Sinha, and A. Sepahvand, "Improved design optimization for high-efficiency matching networks," *IEEE Transactions on Power Electronics*, Vol. 33, 37–50, 2017.
24. Chandravanshi, S. and M. J. Akhtar, "Design of efficient rectifier using IDC and harmonic rejection filter in GSM/COMA band for RF energy harvesting," *Microwave & Optical Technology Letters*, Vol. 59, 681–686, 2017.
25. Xu, X. G., X. X. Zhang, X. Li, and Z. Cheng, "Design of built-in snowflake microstrip antenna built in high-voltage switchgear," *High Voltage Engineering*, Vol. 42, 3207–3213, 2016.